1983

STATISTICAL CHARACTERISTICS OF INSTANTANEOUS DENSE GAS CLOUDS RELEASED IN AN ATMOSPHERIC BOUNDARY LAYER WIND TUNNEL

by

Robert N. Meroney[1]

Achim Lohmeyer[2]

Paper Submitted to

Journal of Boundary Layer Meteorology

September 1983

Accepted October 1983

[1] Professor, Fluid Mechanics and Wind Engineering Program
Civil Engineering Department, Colorado State University,
Fort Collins, Colorado, USA

[2] Consultant Engineer, Karlsruhe, BRD

Revised 31 October 1983

CEP83-84RNM-AL4

Statistical Characteristics of Instantaneous Dense Gas Clouds Released in an Atmospheric Boundary Layer Wind Tunnel

By

Robert N. Meroney
Achim Lohmeyer

Summary:

Wind tunnel experiments were performed to examine the behavior of suddenly released volumes of dense gas in a turbulent shear layer. Instantaneous concentrations were measured with hot-wire katherometers. Multiple replications of each cloud volume, density, and velocity combination produced statistics for plume arrival time, arrival of maximum concentration time, plume departure time and maximum concentrations. Probability distributions and standard deviations of each plume property permit prediction of hazard risks.

1.0 INTRODUCTION:

There now exists a fairly well developed and reasonably satisfactory theory for the prediction of stochastic mean concentrations during turbulent diffusion of dense gases (Blackmore et al., Ermak et al., and Woodward et al. (1982)). Unfortunately for hazard analysis purposes short term ('instantaneous') concentration profiles differ markedly from theoretical mean ones. Pollution models generally predict time average concentrations at fixed points for periods of the order of 1/10 to 1 hour. Randomness does not play a role in these models; hence, they are not suitable to predict the likelihood (or probability) that a single accidental release will produce a hazard at a given time and location.

Although time varying concentration measurements are very limited the statistical characteristics of fluctuating concentrations have been considered by Gifford (1959), Csanady (1973), Netterville (1979), and Wilson (1971, 1982). These analyses are for dispersion in homogeneous stationary shear

layers. The influence of a building on the fluctuating plume has been considered by Li and Meroney (1982); whereas the perturbations caused by the emission of a heavy gas were discussed by Chatwin (1981, 1982).

This paper reports laboratory measurements on the statistical characteristics of instantaneous gas clouds. Section 2.0 reviews the characteristics of the mean behavior of such clouds and suggests a statistical framework for evaluation. Section 3.0 describes the experiment and measurement techniques. Measurements are reported in Section 4.0, and a hazard methodology is applied to hypothetical liquified natural gas (LNG) and propane (LPG) spills in Section 5.0.

2.0 MEAN AND STATISTICAL MEASURES OF DISPERSION BEHAVIOR:

Potential spills or releases of dense hazardous materials may occur in a steady (continuous) or unsteady (instantaneous or finite time) manner. Lohmeyer, Meroney and Plate (1980), Meroney and Lohmeyer (1982, 1983), and Meroney (1983) report laboratory measurements on the unsteady mean behavior of dense gas clouds suddenly released into simulated atmospheric boundary layer. These experiments (Section 2.1) are the foundation for the statistical interpretation provided here in terms of the characteristics proposed in Section 2.2. A hazard model which incorporates the prediction of mean cloud behavior with a verified probability distribution and predictions of concentration standard deviations is proposed in Section 2.3.

2.1 Mean Behavior of Dense Gas Clouds:

The behavior of the ensemble mean of the replicated experiments for the release of dense gas clouds in simulated atmospheric shear layers has been described earlier by Meroney and Lohmeyer (1982, 1983) and Meroney (1983). Sudden release of a dense gas near the ground is accompanied by horizontal

spreading caused by gravitational forces. The cloud spreads laterally and upwind as it collapses converting potential energy into the kinetic energy of a gravity front. The portion of the cloud moving upwind slows and thickens eventually turning back upon itself and the entire cloud begins to move downwind as it entrains momentum with ambient air. Initially cloud stratification inhibits vertical entrainment and most dilution occurs at the cloud edge associated with breaking of the frontal wave. As gravity driven velocities fall below local wind field speeds background turbulence and wind shear begin to enhance entrainment; hence the cloud depth increases.

During the gravity/inertia dominated portion of the cloud lifetime mean concentrations, arrival time, maximum concentration time, and departure time scale with time and space scales equal to $T = V_i^{1/6}(g_i')^{-1/2}$ and $L = V_i^{1/3}$ respectively where $g_i' = g(SG_i - 1)$. The downwind transport of a dense cloud in terms of dimensionless coordinates x^* and t_a^* is shown in Figure 1. Figures 2 and 3 describe plume dilution C_m versus t_a^* and x^* respectively. Plume concentrations decay asymptotically as $(t_a^*)^{-3/2}$ and $(x^*)^{-3}$ during calm situations. For wind shear situations concentration variation with arrival time or distance behaves in a rather irregular manner depending on initial cloud size. For small releases increasing wind speed results in progressively faster concentration decay rates. For the medium and large cloud sizes small wind velocities result in apparently lower concentration decay rates, as the clouds are convected downwind without a proportionally higher rate of dilution. At higher wind speeds the cloud dilutes faster, the decay rates increase and the slope of the curves steepen again.

In Meroney and Lohmeyer (1982) both a volume averaged box model and a depth integrated slab model were developed which reproduced radial cloud dimensions and maximum mean concentrations measured within experimental error

and statistical scatter. The box model did not reproduce the actual vertical and radial variations of height, concentration and velocity in time. Since the box model was designed to reproduce maximum concentrations measured at various spatial locations, then the bulk average concentrations predicted will always be too low, and the entrainment rates a bit high for the reality of local entrainment physics. The slab model reproduced the nuances of roughness and size effects displayed in the experimental data. Considering the simple nature of both models their predictions were respectable. Calculations using the box model are combined with fluctuating plume statistics to predict hazard probabilities in Section 5.0.

2.2 Statistical Properties of a Dense Gas Cloud:

Concentration fluctuations in a dispersing gas cloud are caused by the inherent turbulent character of the medium in which it disperses. The distinctive character of turbulence is its randomness. The results of two separate realizations of a gas cloud dispersion will inevitably be different from one another no matter what precautions are taken to ensure that initial conditions are the same in each realization. Chatwin (1981, 1982) reviewed the basic statistical terminology and relations required to fully describe the variability of dense gas dispersion. He concluded that, at a minimum, one requires the form of the probability density function, $p(C;x,t)$, and the mean, $\overline{C}(x,t)$, and the variance, $\overline{c^2}(x,t)$ of the ensemble of concentration realizations to predict the probability concentrations exceed a given concentration magnitude at x and t.

2.2.1 The Probability Density Function p(C;x,t):

Let the concentration by volume of the dispersing gas at position x and time t be $\chi(x,t)$. The statistical properties of $\chi(x,t)$ can be meaningfully defined only for an ensemble of possible trials. The probability density function (p.d.f.) of χ defines the proportion of the trials for which χ lies between C and C+dC, or

$$p(C;x,t) = \text{prob}(C < \chi(x,t) < C+dC)$$

where prob is an abbreviation for probability. Since concentrations and proportions are essentially positive, the p.d.f. must never be negative. Since $\chi(x,t)$ must lie between zero and one the integral of the p.d.f. must be unity. The ensemble mean concentration may be defined as

$$\bar{C}_m(x,t) = \int_0^{1.0} C \cdot p(C;x,t)dC,$$

and the mean square fluctuation or standard deviation will be denoted by

$$\overline{c^2}(x,t) = \int_0^{1.0} (C - \bar{C}_m(x,t))^2 p(C;x,t)dC.$$

At short times after the release of a dense gas cloud there is a finite possibility that the cloud is unmixed. Similarly as concentrations become small or for locations on the edge of the plume there is a finite possibility that a location has zero concentration. To describe this state of affairs an intermittency factor, G(C;x,t), may be introduced. Thus the probability that the plume is unmixed will be G(1;x,t), the probability that a location is outside the plume or concentrations are zero is G(0;x,t), and the probability that the location is within a mixed plume is (1 - G(1;x,t) - G(0;x,t)). Unfortunately there is almost a complete lack of information on the spatial distribution of the intermittency factor, G(C;x,t). Gifford (1959) has

developed an analytic theory which incorporates the effects of meandering to predict intermittency; however, the theory still requires unknown information about standard deviations of meandering to be complete. During hazard predictions a conservative assumption would be that $(1 - G(1;x,t) - G(0;x,t))$ equals one.

Fackrell and Robins (1980) measured concentration fluctuations and turbulent fluxes for two isolated passive plumes from an elevated and a ground-level source in a simulated neutral, rural, atmospheric boundary layer. Probability density functions were found to follow an exponential distribution for elevated plumes, become log-normal as the plume approached the ground, and near the ground the distributions were very close to Gaussian. This distribution function is strongly affected by the degree of mixing and the presence of a surface.

Csanady (1973) proposed that concentration fluctuations are log-normally distributed about the mean for a continuous ground-level point source and, further, that the distribution is a function of the logarithmic standard deviation only. Wilson (1976) measured concentration fluctuations on a sharp-edged building surface for a source released from different roof vent locations. He reported that the concentration statistics are in good agreement with the log-normal probability distribution and the fluctuation intensity decreases as distance from the vent increases. Li and Meroney (1983) also concluded that the log-normal distribution is a reasonable approximation in a building wake flow when it is assumed that the intermittency factor, $(1-G(1;x,t) - G(0;x,t))$ equals one for every location in the wake.

Since the range of concentrations, C, is limited to between zero and one, it is frequently suggested that the p.d.f. is normally distributed at middle range concentrations and is log-normally distributed at the two ends of the

concentration range. Both distributions are uniquely defined in terms of their mean values and standard deviations. The normal or Gaussian distribution is

$$p(C) = 1./(2\pi\overline{c^2})^{0.5}\exp(-(C - \overline{C_m})^2/(2\ \overline{c^2}))$$

and the form of the log-normal distribution is

$$p_{ln}(C) = 1./((2\pi)^{0.5}\sigma_1 C\ \exp(-(\ln(C/C_{med}))^2/(2\sigma_1^2))$$

where σ_1 is the log-normal standard deviation and C_{med} is the median concentration, or

$$\sigma_1 = \ln(\overline{c^2}/\overline{C_m}^2 + 1)$$

and

$$C_{med} = \overline{C_m}/(1 + \overline{c^2}/\overline{C_m}^2)^{0.5}.$$

Measured probability distributions indeed appear to be a combination of normal, log-normal and intermittency distributions. A set of measurements taken at different locations in a fluctuating plume might appear as shown in Figure 4.

2.2.2 The Variance of Concentration Fluctuations:

As we have just seen the concentration variance, $\overline{c^2}$, is important evidence in fixing the p.d.f.. Wilson et al. (1982) found that the maximum root mean square to mean concentration ratio, $(\overline{c^2})^{0.5}/\overline{C_m}$, generally lies between 0.6 and 0.4 for a ground level neutral density source depending on downwind distance. They also reported vertical profiles of variance which have a max-

imum displaced slightly above the ground surface. They observed that strong variation of variance near the surface can pose difficulties in hazard assessment because variation of receptor height of only a few meters can significantly change the predicted variance. Plume density is also expected to modify distributions and magnitudes of the variance. Chatwin (1981) argued that for suddenly released sources of gases the normalized variance will be inversely proportional to local mean concentration, i.e.

$$\overline{c^2}/\overline{C_m}^2 = \text{const}/\overline{C_m}.$$

Eventually molecular diffusion will reduce $\overline{c^2}$ to zero as time increases. In addition the observations of Wilson et al. (1982) suggest there is an upper limit to this relation.

2.2.3 Predicting Probability of a Hazardous Situation:

When a gas cloud contains toxic, flammable, bacteriological or odorous material one is interested not only in the average levels of concentration but in their instantaneous magnitudes. In particular one is concerned with the total probability, $\mathbb{P}(x)$, that $\chi(x,t)$ resides between limits (of ignition, hazard, etc.) C_1 to C_2, where

$$\mathbb{P}(x) = \int_{C_1}^{C_2} p(C;x)dC.$$

When the p.d.f. is well approximated by a Gaussian curve with mean and variance known, then

$$\mathbb{P}(x) = 1/(\pi)^{0.5} \int_{s_1}^{s_2} \exp(-\xi^2)d\xi$$

where

$$s_1 = (C - C_1)/(2\overline{c^2})^{0.5} \quad \text{and}$$

$$s_1 = (C - C_2)/(2\overline{c^2})^{0.5} \quad \text{and}$$

$\mathbb{P}(x)$ can be evaluated using standard error function tables. For ignitable gases like methane and propane the limiting values are $C_1 = 0.05$ and $C_2 = 0.15$ and $C_1 = 0.022$ and $C_2 = 0.095$ respectively. Alternatively it is possible to predict concentration levels from the p.d.f., mean concentration, and variance information which will not be exceeded more than some prespecified percentage of time. For example for a normal p.d.f. the peak to mean ratio, $C_P/\overline{C_M}$, suggests realizations of $\chi(x,t)$ will exceed $C_P = \overline{C_M} + 1.65(\overline{c^2})^{0.5}$ only 5 percent of the time. Similar expressions for log-normal p.d.f. are summarized by Chatwin (1981).

3.0 EXPERIMENTAL CONFIGURATION:

An experiment was designed to examine the dispersion of instantaneous volumes of dense gas released at ground level in a wind tunnel capable of simulating the atmospheric boundary layer. The gases were released as initially half-cylindrical clouds, and the concentrations were monitored by aspirated-hot-wire katherometer.

3.1 Wind Tunnel and Source Generation Equipment:

The open-circuit wind tunnel used had a test section 0.5 m high, 1.5 m wide, and 5 m long. At the tunnel entrance was a dense honeycomb and a vortex spire/barrier flow-conditioner arrangement which produced a 30 cm deep turbulent shear layer that reached equilibrium and remained stationary over the final 3 meters of the test section. A 14 cm x 16 cm x 12 cm deep container of water was maintained flush to the test section floor 2.5 meters from the

entrance as noted in Figure 5. The rectangular box contained an apparatus to fill a half cylinder cup with dense gas, to raise the filled cylinder above the water surface until it stood exposed to the wind, but isolated by a water seal, and to suddenly rotate the horizontal cylinder about its axis, leaving a volume of dense gas almost motionless above the water surface. The cup rotated 180^{o} in less than 1/20 second. A small magnet on the cup activated a reed switch which provided a voltage pulse to timing instrumentation.

3.2 Concentration Measurements:

Dense-gas concentrations were measured with an aspirated-hot-film anemometer (katherometer) constructed from a DISA 55E07 mass-flow transducer. The aspiration velocity at the 1 mm diameter probe tip was set at less than 0.1 m/sec to assure approximately isokinetic sampling of the cloud. All tests were corrected for a slight time lag required for the sample to travel through the probe to the detection wire. Extensive tests indicate such a probe has a flat frequency response to 150 Hertz, concentration sensitivity to 0.10 percent, and resolution within 5 percent of a measurement.

During each realization of a volume release the katherometer response was registered at a fast response chart recorder. Each sample point was recorded a minimum of five times. Time response was displayed within a resolution of $t = 0.1$ sec ($t^{*} < 3$).

4.0 STATISTICAL CHARACTERISTICS OF LABORATORY MEASUREMENTS:

Experiments were performed with dichlorodifluromethane (CCl_2F_2) (Specific Gravity = 4.17) and 35, 165, and 450 cm^3 initial volumes; hence length scales for the dense releases were L = 3.3, 5.5, and 7.7 cm; whereas time scales were T = 0.032, 0.042, and 0.049 seconds respectively. Wind tunnel velocities at a 10 cm reference height were varied from 0 to 1.0 m/sec. For one release

condition (V_i = 450 cm^3, u_R = 0.4 m/sec, x = 0.4 m, and z = 0.002 m) one hundred independent replications were performed.

4.1 Probability Distributions for C_m, t_a, t_m, and t_d:

The time response of the aspirated hot-wire probe during a typical sequence of measurements is shown in Figure 6. Typical katherometer response curves are displayed in Figure 7a and 7b. Data recorded from each response curve includes the arrival time, t_a, the arrival time of the concentration maximum, t_m, the departure time of the cloud, t_d, and the maximum concentration, C_m. Each scenario was repeated about five times and the average dimensionless value of each measure used to create Figures 1 to 3.

The single release scenario of a large cup, u_R = 0.4 m/sec, and a location of x = 0.4 m and z = 0.002 m was repeated about 100 times. A plot of the probability distribution indicated that t_a^* and C_m were normally distributed about their means. Plots of t_m^* and t_d^* produced log-normal distribution behavior. Ten of the katherometer response replications are plotted together in Figure 8. Figure 9 superimposes the p.d.f. for each variable on a plot of C versus t^*.

4.2 Concentration Variance Behavior:

The concentration variance near the wall ranged from 0.2 to 0.4; thus, single measurements could deviate markedly for these highly transient instantaneous source situations from the ensemble means. Indeed, assuming a normal distribution, a single measurement may deviate from the ensemble mean by $\pm$33 to 66 percent with a probability of 5 percent. Accordingly it appears possible to interpret entrainment parameters which vary by an order of magnitude if one calibrates analytic or numerical models based on outlying values from single field sample realizations.

Close to the source location, i.e. $x^* < 4$, maximum concentrations vary with height in a similar manner. One can conclude that in this region the cloud is still governed by gravitational dynamics alone. Figures 10, 11, and 12 display vertical profiles of mean concentration, $\overline{C}_m$, and variance ratio, $(\overline{c^2})^{0.5}/\overline{C}_{mo}^2$, for three downwind locations. Beyond $x^* = 5$ the effects of source size and wind speed are noticeable. Higher wind speeds generally result in higher concentrations, but even higher speeds reduce concentrations. As wind shear increases there is also a tendency for the associated background turbulence to mix gases to distances further from the wall. Vertical profile shape varies; however, there is a noticeable tendency to pass from exponential to Gaussian, and then to an elevated nose profile as velocity increases. Since only five replications were used to calculate variances and means error bounds about these values are large; nonetheless, from the large number of cases considered one may conclude mean concentration variance are both distributed over similar heights over a range of wind speed and source conditions. Also larger source volumes slump to lower heights when scaled by the cube root of the initial source volume.

The concentration variance ratio, $(\overline{c^2})^{0.5}/\overline{C}_m$, is plotted versus dimensionless downwind distance, x^*, in Figure 13. Notice that for the smallest cup (smallest density effects) the ratio seems to approach a limit between 0.5 and 0.35 similar to the behavior of passive plumes discussed by Wilson et al. (1982). Larger volumes generate larger gravity forces and the upper limit of the ratio declines to levels between 0.2 and 0.1.

Finally the variance ratio for all ground level measurements are plotted versus their associated mean concentration level in Figure 14. The algorithm suggested by Chatwin (1981) in Section 2.2.2 provides an upper bound to 95

percent of the data when the constant equals 0.02, i.e.

$$\overline{c^2}/\overline{C_m}^2 = 0.02/\overline{C_m}$$

This expression may be rather conservative due to the error associated with using only five replications to predict concentration variances. In addition there appears there may be a cloud scale (or Ri_*) effect reducing the variance ratio magnitude.

5.0 HAZARD CALCULATIONS FOR LNG AND PROPANE SPILLS:

Evidence now exists that concentrations are distributed about their mean values in a Gaussian manner, variances for dense gas clouds obey a Chatwin style relation, and mean concentrations may be reliably predicted by simple numerical box or slab models. This information has been used together with the approach discussed in Section 2.3 to produce hazard estimates for typical LNG and propane spill situations. (See Figures 15 and 17.)

Figure 15 predicts the probability that peak concentrations during a release situation will lie within a flammable range. In this instance it is assumed that ignition will occur. If the ensemble average peak concentration, $\overline{C}_m$, exceeds the LFL it may be presumed that flammable gases will exist at the location sometime; hence given the presence of a continuous ignition source ignition could occur. The interesting question of course will be if $\overline{C}_m$ is less than LFL what is the likelihood that C_m will exceed the LFL.

Fay and Lewis (1975) constructed a figure for the probability of flammable composition from measurements made by ESSO during the Matagarda Bay LNG spills in 1971. An LNG jet was pumped out over the side of a ship onto the water. Fay and Lewis calculated the percentage of time that gas concentrations exceeded average values. Their ignition figure shows a lower peak

probability and a correspondingly wider curve than in Figure 15. This reflects their use of a lognormal probability distribution with larger variance. The large variance results from the use of near zero concentration data taken at off axis locations where $\sqrt{\overline{c'^2}}/\overline{c}_m$ may approach very large values due to plume meander.

5.1 Probability of Ignition for China Lake Burro Test 8:

During the Burro 8 Field Trial at China Lake Naval Weapons Center 28.4 m^3 of LNG was released at a rate of 16.0 m^3/min onto a small water pond. The wind speed was 1.8 $\pm$ 0.3 m/sec and decreasing at a 1 m height, while the atmospheric stability was slightly stable. Humidity was measured to be 5% upwind of the spill and air temperature was 33°C.* This spill displayed the most gravity dominated behavior of those performed. (See Koopman, et. al. (1982), and Meroney and Neff (1981), for a discussion of field data.)

The box model described by Meroney (1983) was run for Burro 8 initial conditions for both adiabatic entrainment of dry air and mixed-convection heat transfer plus entrainment of air at 20% humidity. The mean maximum concentrations of methane, $\overline{C}_m$, versus downwind distance, x, is plotted in Figure 16. Apparently water vapor condensation and surface heat transfer play minor roles in the dispersion process before reaching the lower flammability limit of 5% (LFL). Superimposed upon the figure is a prediction of the probability of ignition calculated in the manner discussed in Section 2.3. Ignition probability exceeds 5% between distances of 65 to 900 meters; although the mean concentration falls below 0.05 beyond 400 meters. Note that the probability of ignition, $\mathcal{P}$, only indicates the likelihood that a flammable methane-air

---

* Since the plume mixes violently over the pond it is likely that downwind of the pond the humidity is higher (20%).

mixture will arrive at a given downwind location. The flame may be convected downstream and eventually extinguished, or it may be propagated against the general direction of the flow with subsequent total light-up of the entire cloud. The most striking feature of the figure is that there is no close connection between the observed flammable boundary and the surface on which the mean concentration is equal to the LFL.

5.2 Prediction of Propane Cloud Behavior:

This section uses the numerical box model program described in Meroney and Lohmeyer (1983) to calculate a range of hazard distances for instantaneous releases of gas clouds produced from the sudden vaporization of propane (LPG). The distances calculated to mean concentration LFL or to a probability of ignition, ℙ, equal to 5% are compared in Table 1 to recommendations for evacuation areas provided by the Chemical Hazard Response Information System (CHRIS) prepared by the Department of Transportation, Coast Guard, U.S.A. The CHRIS methodology is described by Parnarouskis, Flessner, and Potts (1980). The CHRIS program calculates the LFL regions based on a neutral-density gaussian plume model approach.

Table 1 compares hazard zones for propane spills ranging from 0.1 to 1000 tons into a low-wind-speed neutral-stratification environment. Notice that the CHRIS model expects a cigar shaped plume extending fairly far downwind. The CHRIS model assumes the plume is convected as $x = u_R t$, but the sudden collapse of a cold cloud will place the majority of the gas near the ground, where the wind speeds are very low. Thus the Coast Guard model overestimates plume transport, but underestimates plume width substantially. The dense gas box model reveals that the plume spreads rapidly outward from the source into

Table 1. Propane (PG) Hazard Assessment▲

Spill Sizes (short tons)	(kg)	CHRIS LFL (m)	CHRIS Half-width (m)	CHRIS t_a (min)	BOX LFL_1* (m)	BOX LFL_2Δ (m)	BOX Half-width$_1$* (m)	BOX Half-width$_2$Δ (m)	BOX $T_{a\,1}$* (min)	BOX $T_{a\,2}$Δ (min)
0.1	91	18	8	0.1	30	46	28	40	0.50	1.17
1.0	907	152	18	1	66	100	60	85	1.00	1.67
10.0	9072	602	38	4	140	210	127	185	1.25	2.50
100.0	90720	1389	98	9	300	450	275	400	2.00	3.67
1000.0	907200	3195	200	21	650	950	600	850	2.67	5.33

▲ Revised Table 1 from Meroney and Lohmeyer (1983)

* LFL_1 based on distance to $\bar{C}_m = 0.02$ ($\mathbb{P} = 0.30$)

Δ LFL_2 based on log-normal probability distribution of C_m, $\overline{C'^2} = 0.02\,\bar{C}_m$, and $\mathbb{P}$ ignition ≤ 0.05, i.e. $\bar{C}_m = 0.007$

$u \cong$ 1-5 knots, D stability

lapse of a cold cloud will place the majority of the gas near the ground, where the wind speeds are very low. Thus the Coast Guard model overestimates plume transport, but underestimates plume width substantially. The dense gas box model reveals that the plume spreads rapidly outward from the source into more of a pancake shaped configuration. Substantial advection even occurs upwind.

Making safety decisions based on the mean concentration levels is unwise, since the probability of ignition remains high (P = 30%) for mean concentrations only slightly below 0.022. To reach ignition probabilities below 5% requires distances 50% greater than those where the mean LFL concentration occurs.

ACKNOWLEDGEMENTS:

The author wishes to acknowledge support from the Institute Wasserbau III, University of Karlsruhe, F.R.G., the von Humboldt Foundation, F.R.G., and the Gas Research Institute, U.S.A.

6.0 REFERENCES:

Blackmore, D. R., Herman, M. N., and Woodward, J. L. (1982), Heavy Gas Dispersion Models, J. of Hazardous Materials, Vol. 6, Nos. 1 and 2, pp. 107-128.

Chatwin, P. C. (1981), The Statistical Description of the Dispersion of Heavy Gas Clouds, Report to Health and Safety Executive under Contract No. 1189/01.01, Univ. of Liverpool, U. K., 140 pp.

Chatwin, P. C. (1982), The Use of Statistics in Describing and Predicting the Effects of Dispersing Gas Clouds, J. of Hazardous Materials, Vol. 2, Nos. 1 and 2, pp. 213-230.

Csanady, G. T. (1973), Turbulent Diffusion in the Enviroment, D. Reidel Publishing Company, Boston-U.S.A., 248 pp.

Ermak, D. L., Chan, S. T., Morgan, D. L., and Morris, L. K. (1982), A Comparison of Dense Gas Dispersion Model Simulations with Burro Series LNG Spill Test Results, J. of Hazardous Materials, Vol. 2, Nos. 1 and 2, pp. 129-160.

Fackrell, J. E., and Robins, A. G. (1980), Concentration Fields Associated with Emissions from Point Sources in Turbulent Boundary Layers: Part III. Concentration Fluctuations and Fluxes, Central Electricity Generating Board, Memorandum MM/MECH/TF 260, Marchwood Engineering Laboratories, Southhampton, U. K., 51 pp.

Fay, J. A. and Lewis, D. H. Jr. (1975), The Inflammability and Dispersion of LNG Vapor Clouds, Fourth International Symposium on Transport of Hazardous Cargoes by Sea and Inland Waterways, Jacksonville, Florida, 26-30 October, pp. 489-498.

Gifford, F. A. (1959), Statistical Properties of a Fluctuating Plume Dispersion Model. Atmospheric Diffusion and Air Pollution, ed. F. N. Frenkiel and P. A. Sheppard, Advances in Geophysics, Vol. 6, pp. 117f.

Koopman, R. P., Cederwall, R. T., Ermak, D. L., Goldwire, H.C. Jr., Hogan, W. J., McClure, J. W., McRae, T. G., Morgan, D. L., Rodean, H. C., and Shinn, J. H. (1982), Analysis of Burro Series 40 m^3 LNG Spill Experiments, J. of Hazardous Materials, Vol. 6, Nos. 1 and 2, pp. 43-84.

Li, W. W., and Meroney, R. N. (1983), Gas Dispersion Near a Cubical Model Building, Part II: Concentration Fluctuation Measurements, J. of Wind Engineering and Industrial Aerodynamics, Vol. 12, No. 1, pp. 35-47.

Lohmeyer, A., Meroney, R. N., and Plate, E. J. (1980), Model Investigations of the Spreading of Heavy Gases Released from an Instantaneous Volume Source at the Ground, Air Pollution Modeling and Its Applications, Vol. 1, edited by C. de Wispelaere, Plenum Publishing Corp., pp. 433-448.

Meroney, R. N. (1983), Unsteady Behavior of a Simulated LNG Vapor Cloud Suddenly Released into a Wind-tunnel Boundary Lyer, Proceedings of American Gas Association, Transmission Conference, May 2-4, 1983, Seattle, Washington, 21 pp.

Meroney, R. N. and Lohmeyer, A. (1982), Gravity Spreading and Dispersion of Dense Gas Clouds Released Suddenly into a Turbulent Boundary Layer, Gas Research Institute Research Report GRI-81/0025, Chicago, Illinois, U. S. A., 220 pp.

Meroney, R. N. (1983), Prediction of Propane Cloud Dispersion by a Wind-tunnel-data Calibrated Box Model, J. of Hazardous Materials, accepted for publication, 33 pp.

Meroney, R. N., and Neff, D. E. (1981), Physical Modeling of Forty Cubic Meter LNG Spills at China Lake, California, Air Pollution Modeling and Its Applications, Vol. 1, edited by C. de Wispelaere, Plenum Publishing Corp., pp. 24-27.

Netterville, D. D. J. (1979), Concentration Fluctuations in Plumes, Syncrude Environmental Research Monograph 1979-4, Syncrude Canada Ltd., Edmonton, Canada, 288 pp.

Parnarouskis, M. C., Flessner, M. F., and Potts, R. G. (1980), A Systems Approach to Chemical Spill Response Information Needs, Hazardous Chemical - Spills and Waterborne Transportation, edited by S. S. Weidenbaum, American Institute of Chemical Engineers Symposium Series, Vol. 76, No. 194, pp. 32-41.

Wilson, D. J. (1976), Contamination of Building Air Intakes from Nearby Vents, Report No. 1, Department of Mechanical Engineering, University of Albeta, Edmonton, Canada, 126 pp. or ASHRAE Trans., Vol. 82, Part 1, pp. 1024-1038.

Wilson, D. J. (1981), Along-wind Diffusion of Source Transients, Atmospheric Environment, Vol. 15, pp. 489-495.

Wilson, D. J., Robins, A. G., and Fackrell, J. E. (1982), Predicting the Spatial Distribution of Concentration Fluctuations from a Ground Level Source, Atmospheric Environment, Vol. 16, No. 3, pp. 497-504.

Woodward, J. L., Havens, J. A., McBride, W. C., and Taft, J. R. (1982), A Comparison with Experimental Data of Several Models for Dispersion on Heavy Vapor Clouds, J. of Hazardous Materials, Vol. 6, Nos. 1 and 2, pp. 161-180.

7.0 LIST OF SYMBOLS:

Symbols	Definitions
C	Concentration
C_m	Maximum transient concentration
C_{med}	Median concentration
C_1, C_2	Lower and upper flammability limits
C_P	Peak concentration
g'	Modified gravitational constant
$G(C;x,t)$	Intermittency factor
L	Length scale
LFL	Lower flammability limit
LNG	Liquified natural gas
$p(C;x,t)$	Probability density function (p.d.f.)
$p_{ln}(C;x,t)$	Log-normal p.d.f.
$P(x,t)$	Ignition probability
R	Concentration intensity ratio
Ri_*	Richardson number
s_1, s_2	Dimensionless lower and uppe flammability
T	Time scale
t	Time
U	Velocity scale
u	Velocity
u_*	Friction velocity
x	Downwind distance
X	Concentration
σ_1	Log-normal standard deviation
ϕ	Humidity

Symbols	Definition
Subscripts	
a	Arrival time
i	Initial
d	Departure time
m	Maximum
o	Ground level
R	Reference
Superscripts	
---	Ensemble average
*	Dimensionless

8.0 LIST OF FIGURES:

Figure	Title
1	Cloud Transport Distance versus Arrival Time
2	Cloud Dilution versus Arrival Time
3	Cloud Dilution versus Downwind Distance
4	Probability Distribution Functions for Different Ranges of Concentration
5	Experimental Configuration
6	Typical Time Response Characteristics of Katherometer Located at Various Positions Downwind of the Source
7	Replications of Katherometer Response at Various Downwind Locations, V_i = 450 cm^3, u_R = 0.6 m/s
8	Replications of Katherometer Response, V_i = 450 cm^3, u_R = 0.4 m/s
9	Probability Distributions for C_m, t_a^*, t_m^*, and t_d^* Superimposed upon C versus t_a^* Response
10	Vertical Profiles of Mean and Concentration Variance
11	Vertical Profiles of Mean and Concentration Variance
12	Vertical Profiles of Mean and Concentration Variance
13	Concentration Variance Ratio versus Dimensionless Downwind Concentration
14	Concentration Variance Ratio versus Mean Concentration
15	Probability of Ignition of LNG Vapor Cloud versus Mean Maximum Concentration
16	Ignition Probabilities during China Lake Burro 8 LNG Spill, $\overline{C_m}$ and P versus x (meters)
17	Probability of ignition of Propane Cloud versus Mean Maximum Concentration

LIST OF TABLES:

Table	Title
1	Propane (L.P.G.) Hazard Assessment

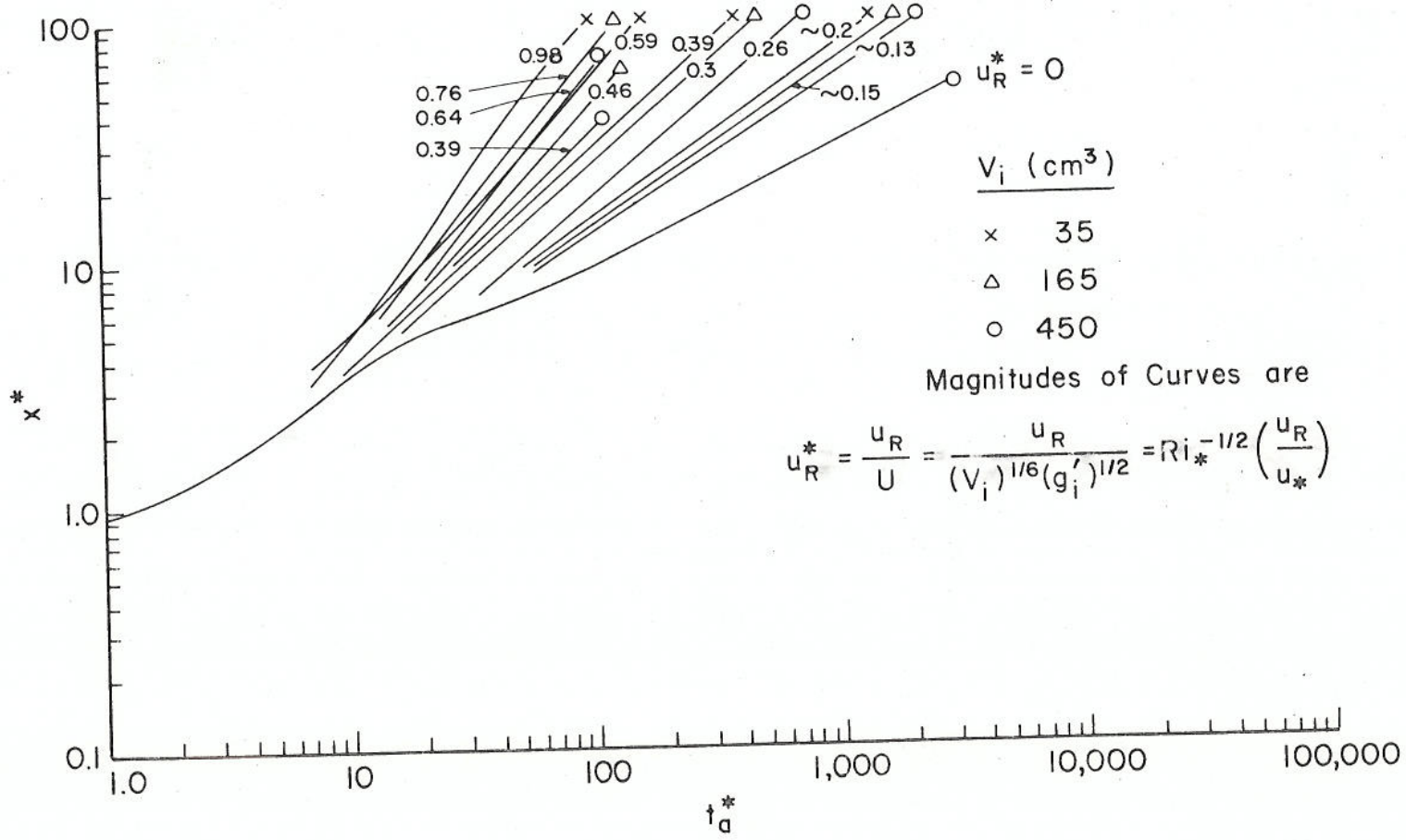

Figure 1. Cloud Transport Distance versus Arrival Time

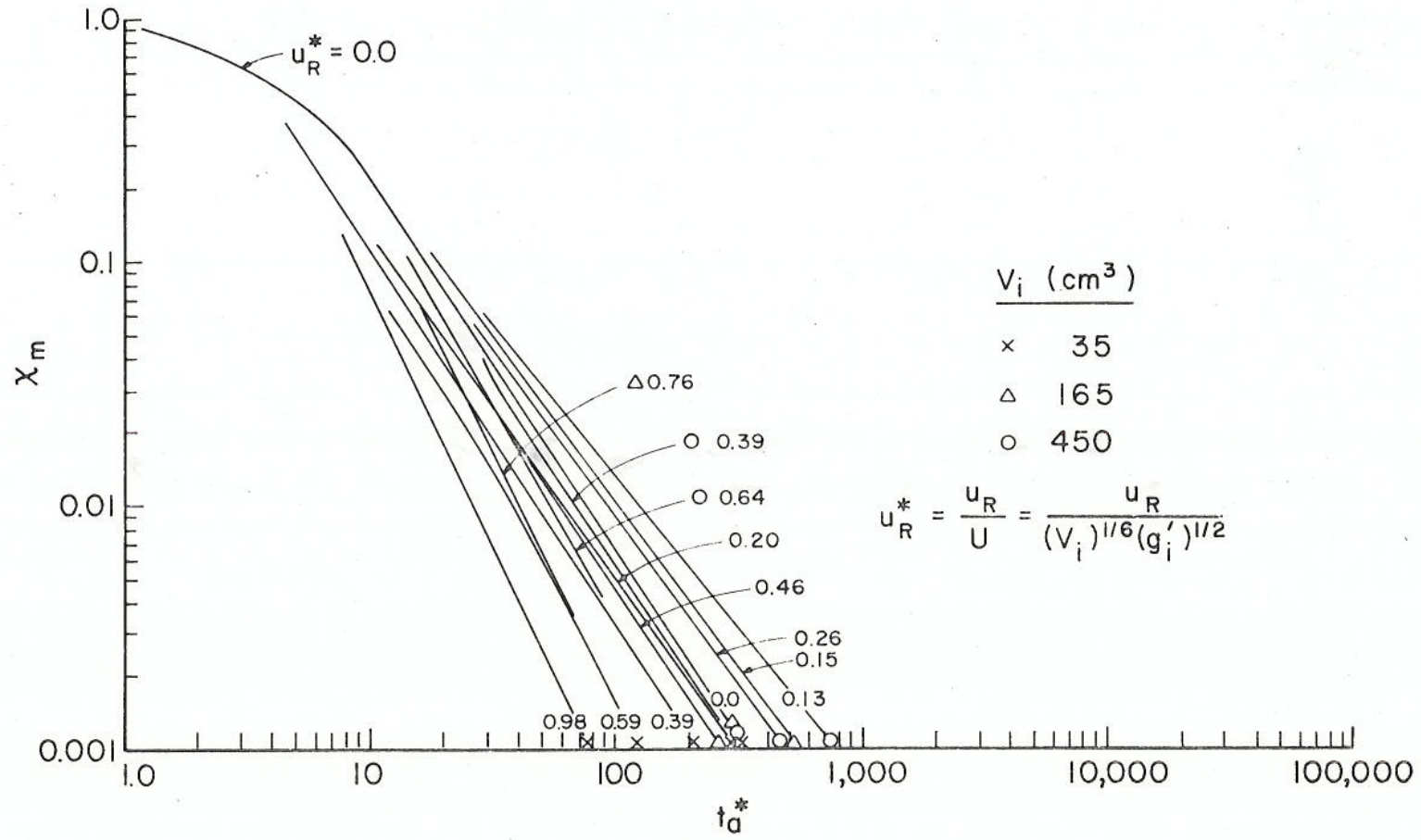

Figure 2. Cloud Dilution versus Arrival Time

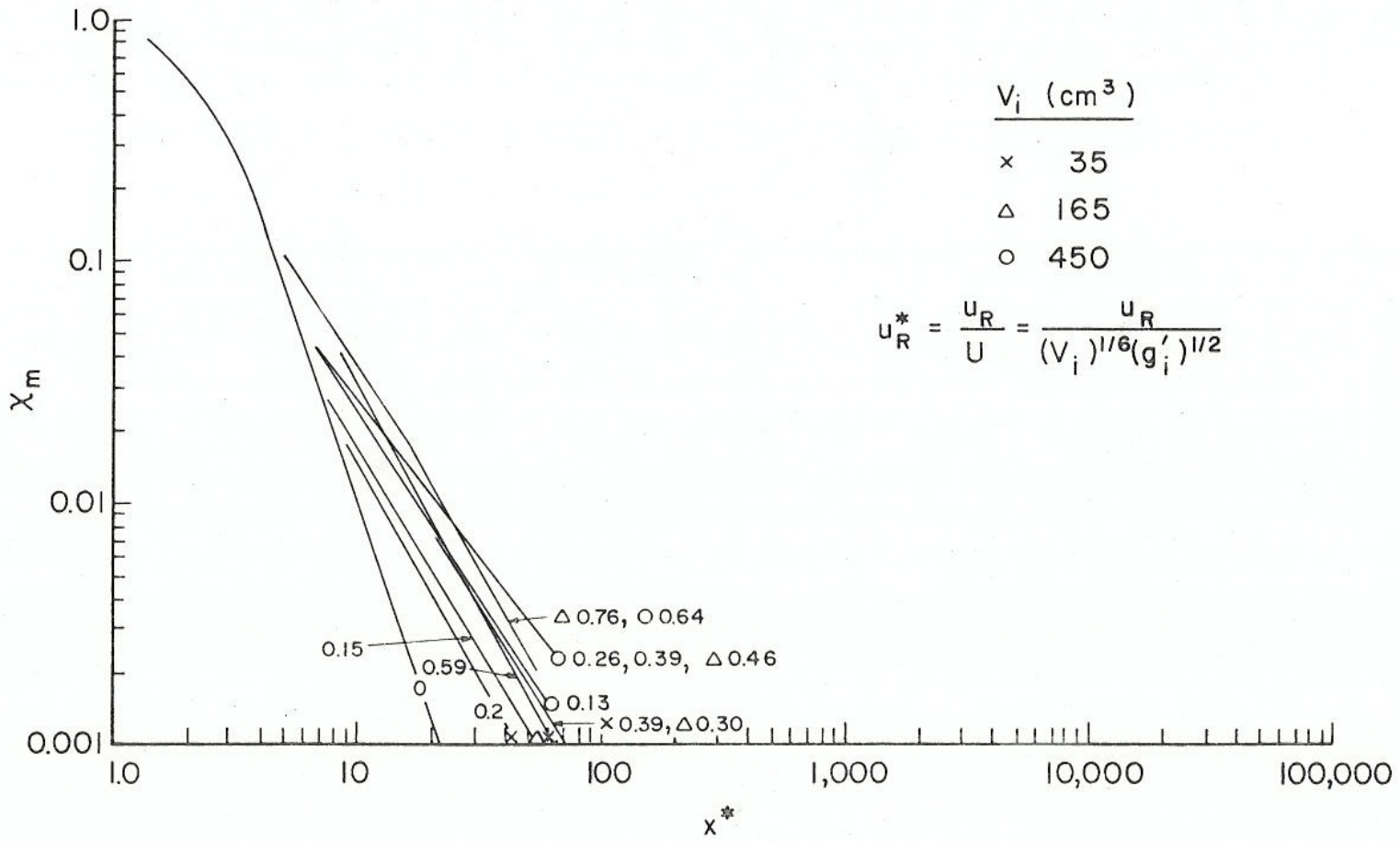

Figure 3. Cloud Dilution versus Downwind Distance

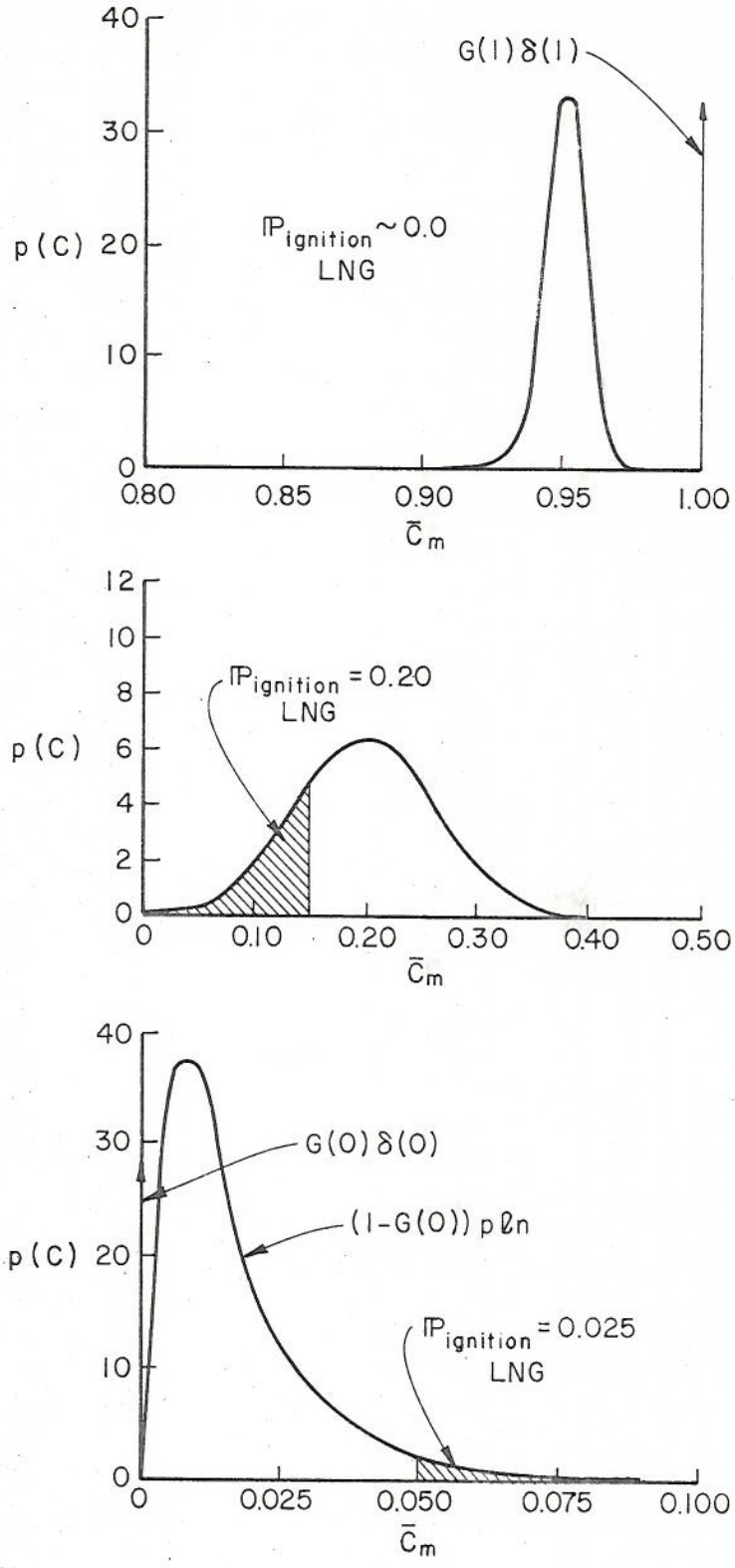

$\bar{C}_m = 0.95$

$G(1) = 0.4$

$\overline{C'^2} = 0.019$

p.d.f. = log normal

$p(C) = G(1)\delta(1) + (1-G)p\ell n(C)$

$\bar{C}_m = 0.20$

$G(1) = G(0) = 0$

$\overline{C'^2} = 0.004$

$p(C) = p_n(C)$

$\bar{C}_m = 0.02$

$G(0) = 0.2$

$\overline{C'^2} = 0.0004$

$p(C) = G(0)\delta(0) + (1-G(0))p\ell n(C)$

Figure 4. Probability Distribution Functions for Different Ranges of Concentration

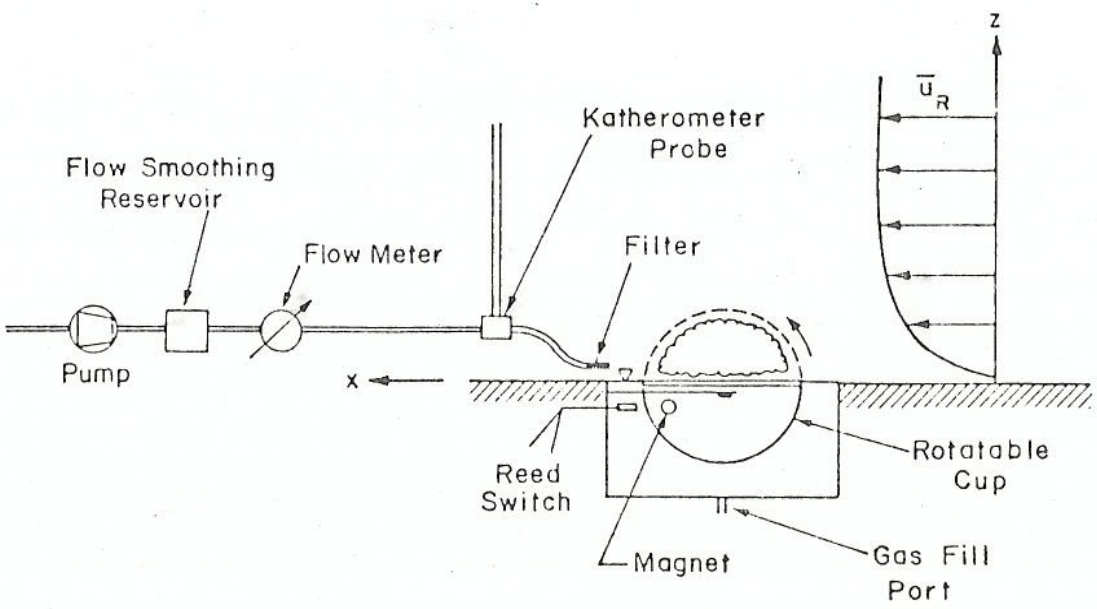

Figure 5. Experimental Configuration

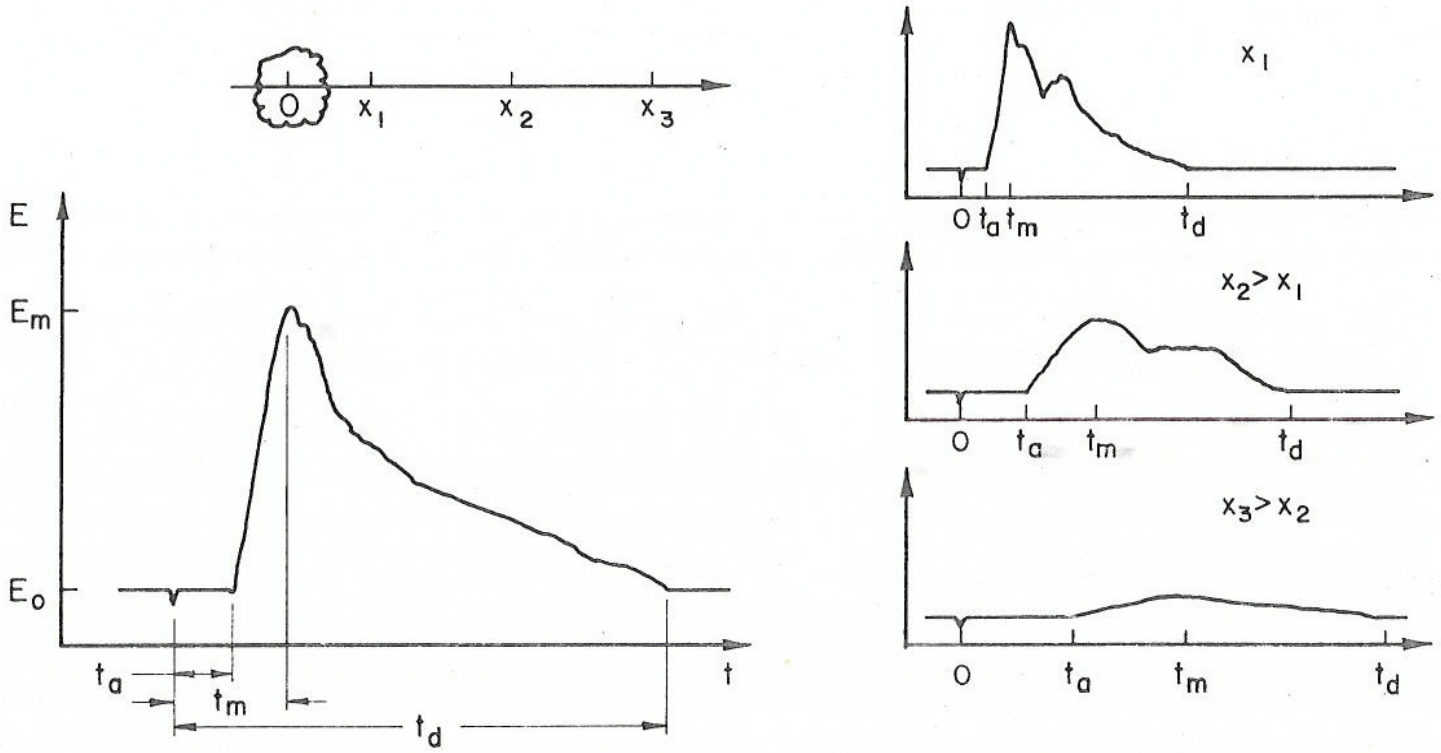

Figure 6. Typical Time Response Characteristics of Katherometer Located at Various Positions Downwind of the Source

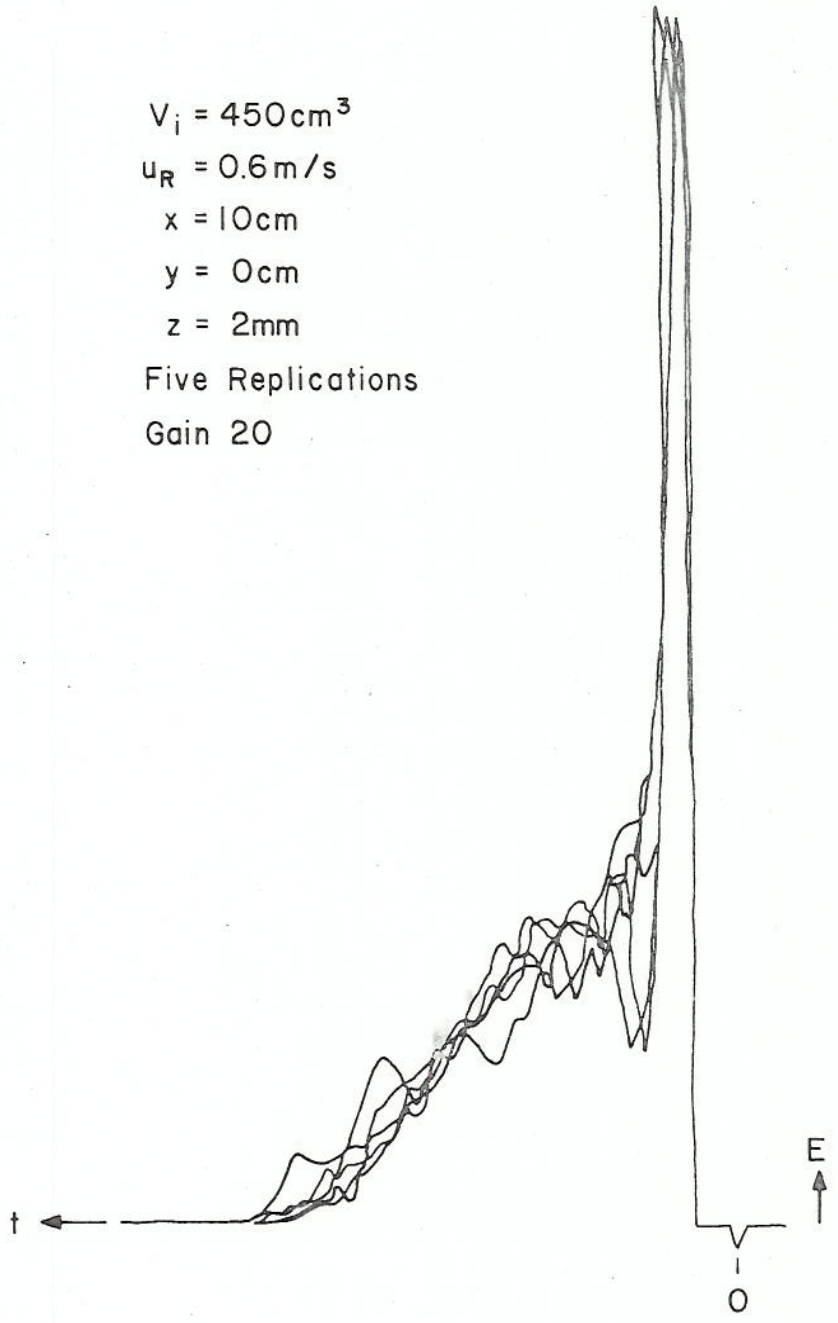

Figure 7a. Replications of Katherometer Response at Various Downwind Locations, V_i = 450 cm^3, u_R = 0.6 m/s

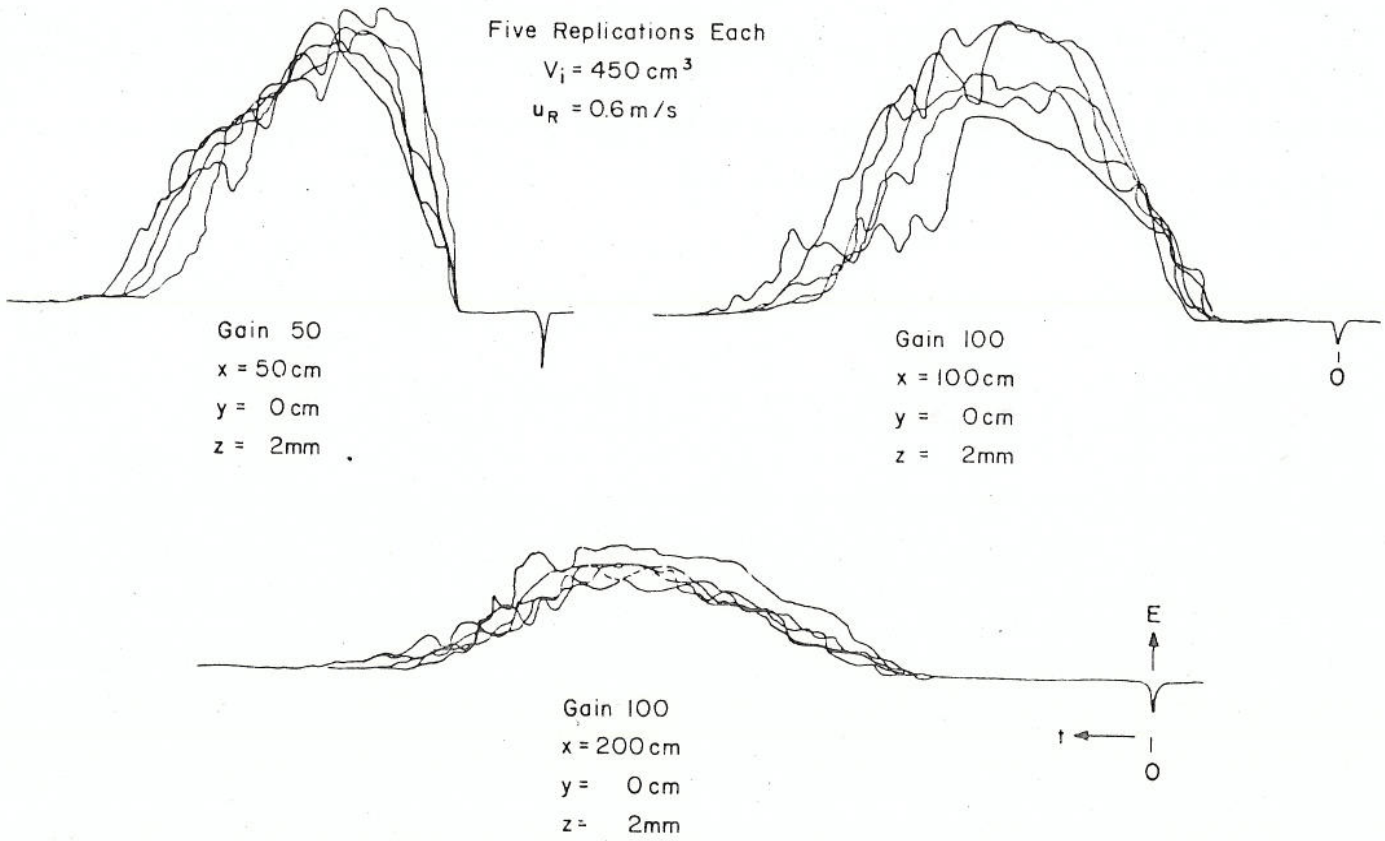

Figure 7b. Replications of Katherometer Response at Various Downwind Locations, V_i = 450 cm^3, u_R = 0.6 m/s

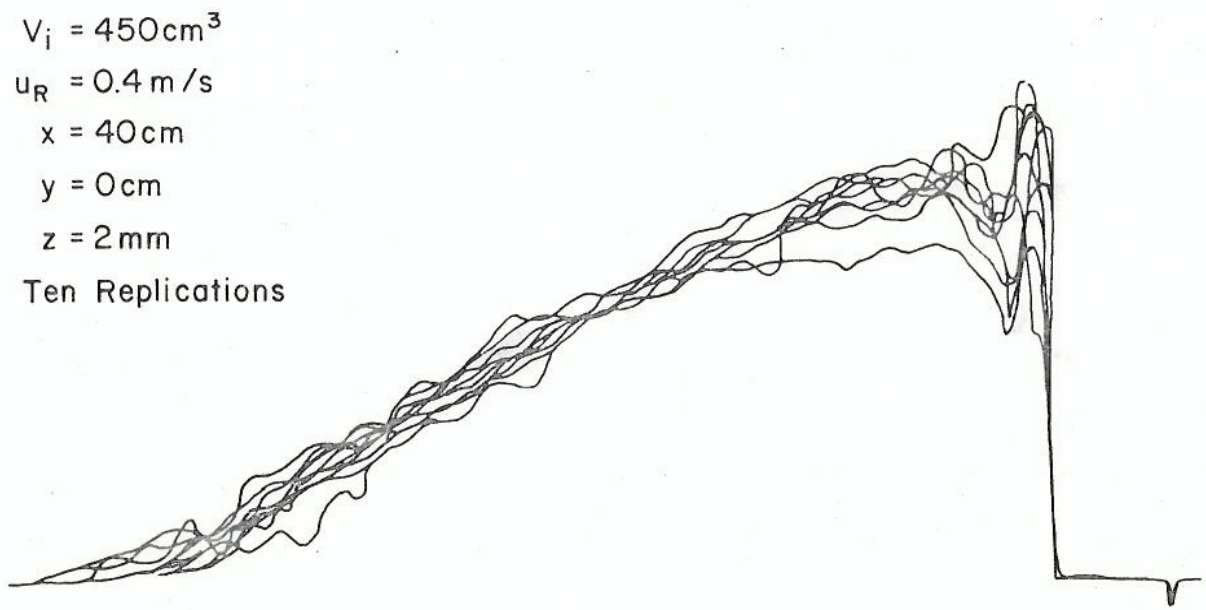

Figure 8. Replications of Katherometer Response, V_i = 450 cm^3, u_R = 0.4 m/s

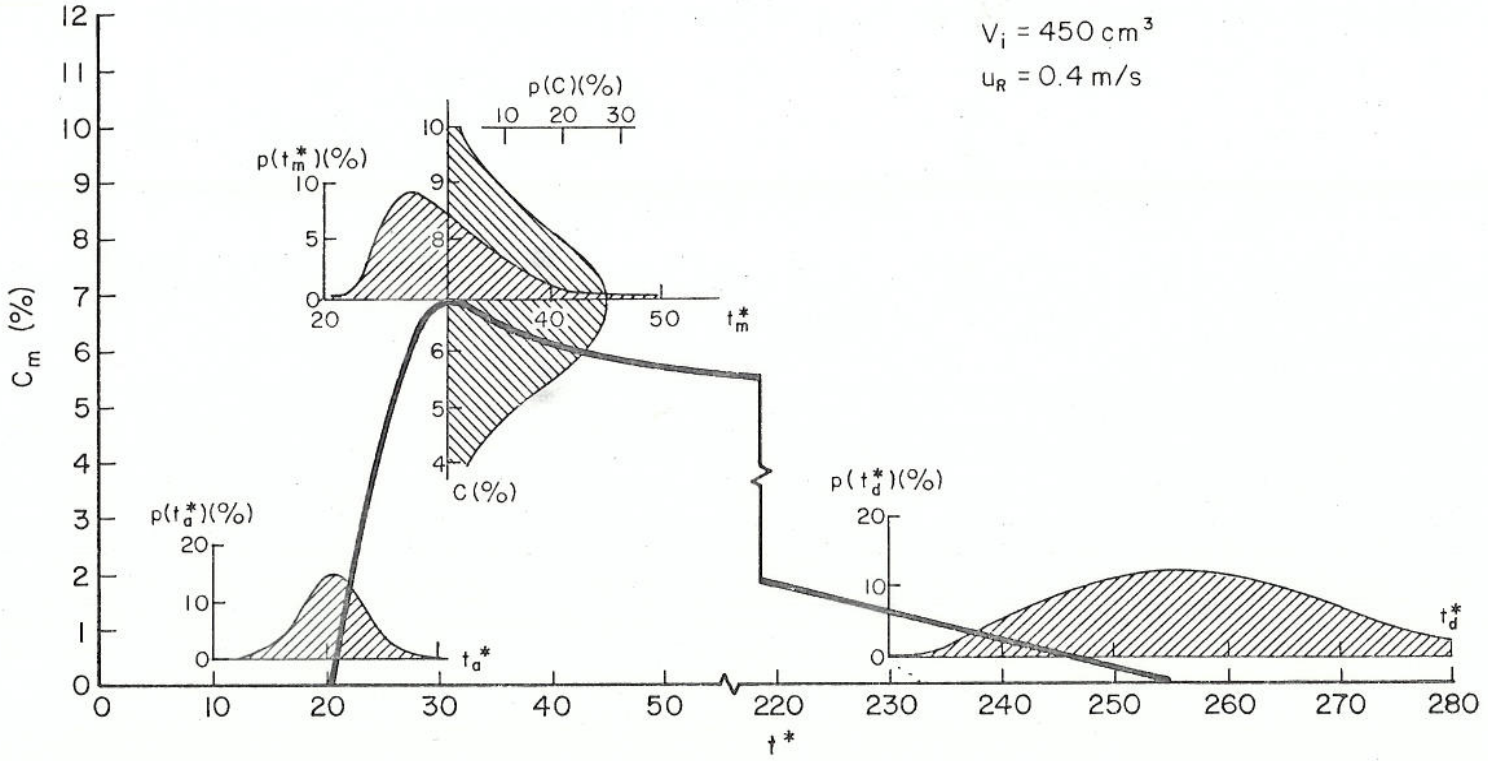

Figure 9. Probability Distributions for C_m, t_a^*, t_m^*, and t_d^* Superimposed upon C versus t_a^* Response

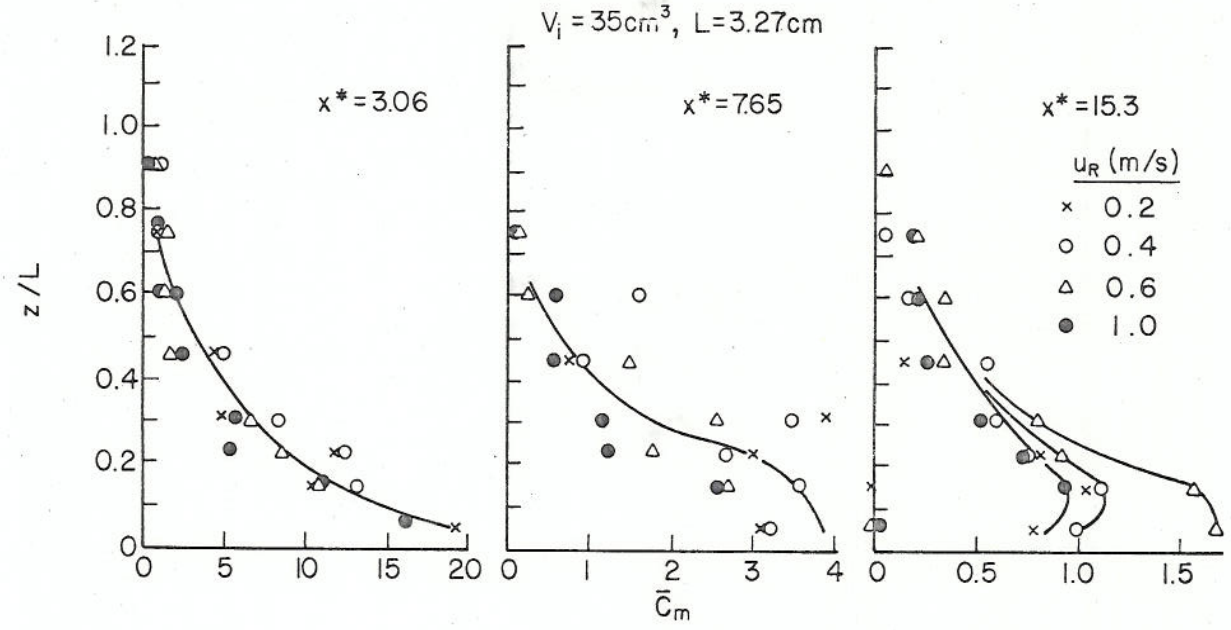

(a)

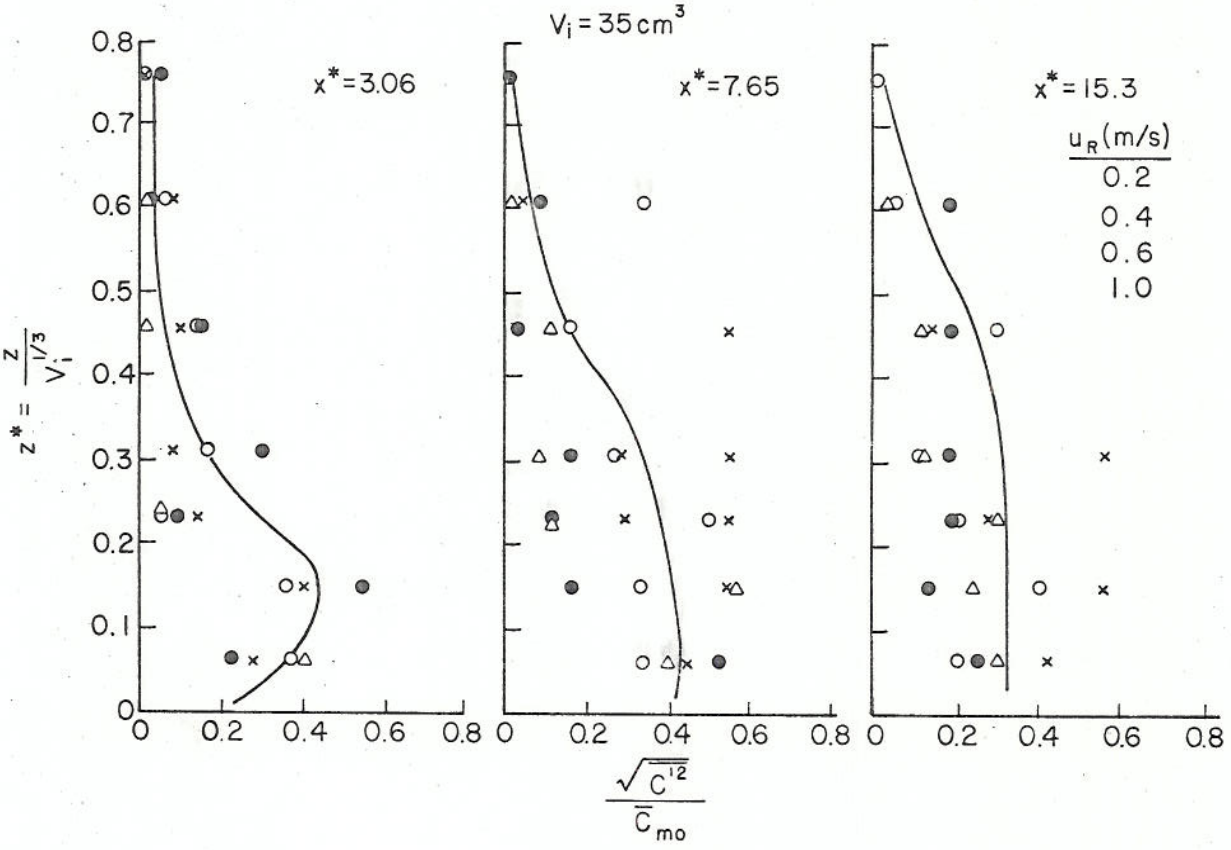

(b)

Figure 10. Vertical Profiles of Mean and Concentration Variance

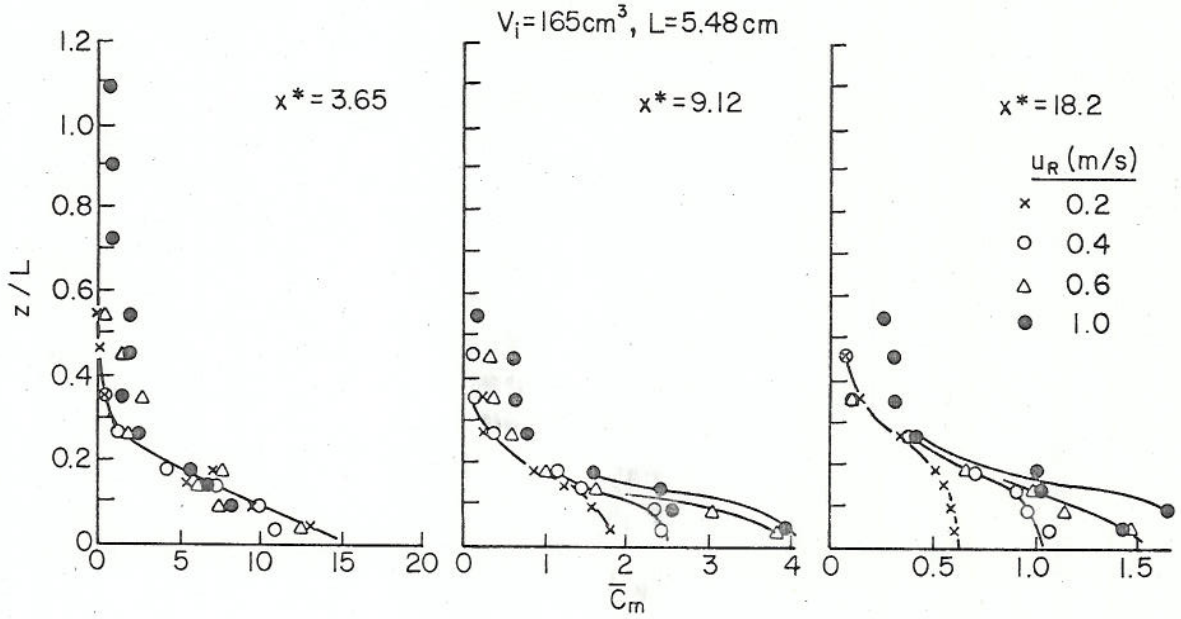

(a)

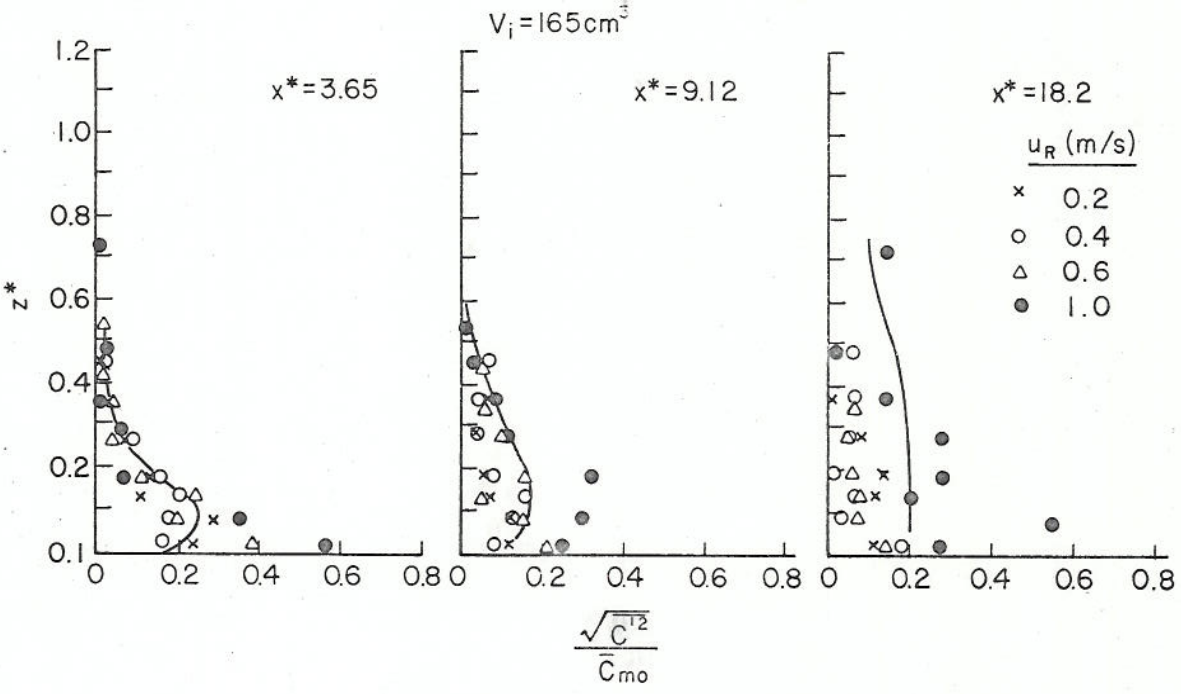

(b)

Figure 11. Vertical Profiles of Mean and Concentration Variance

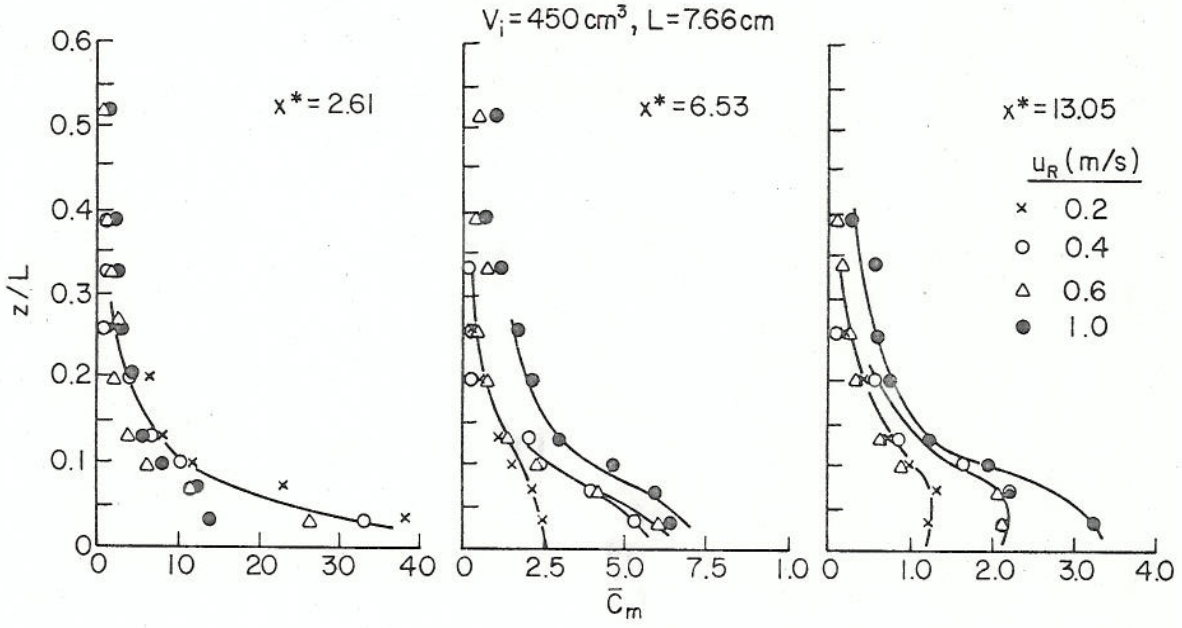

(a)

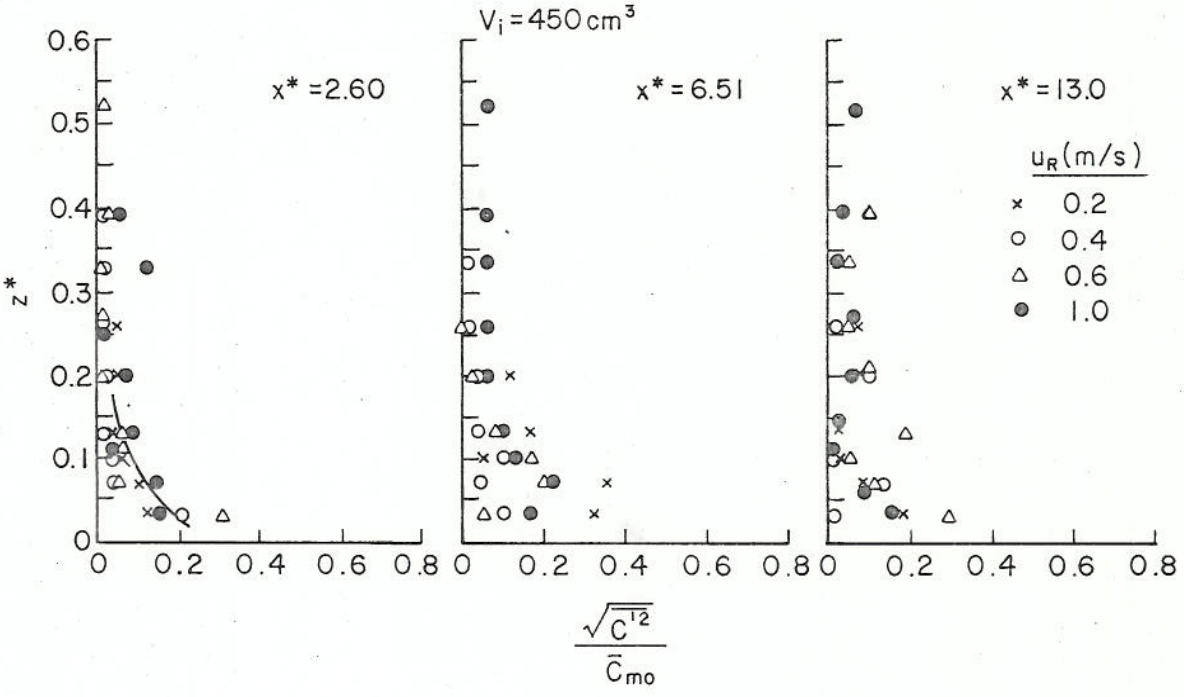

(b)

Figure 12. Vertical Profiles of Mean and Concentration Variance

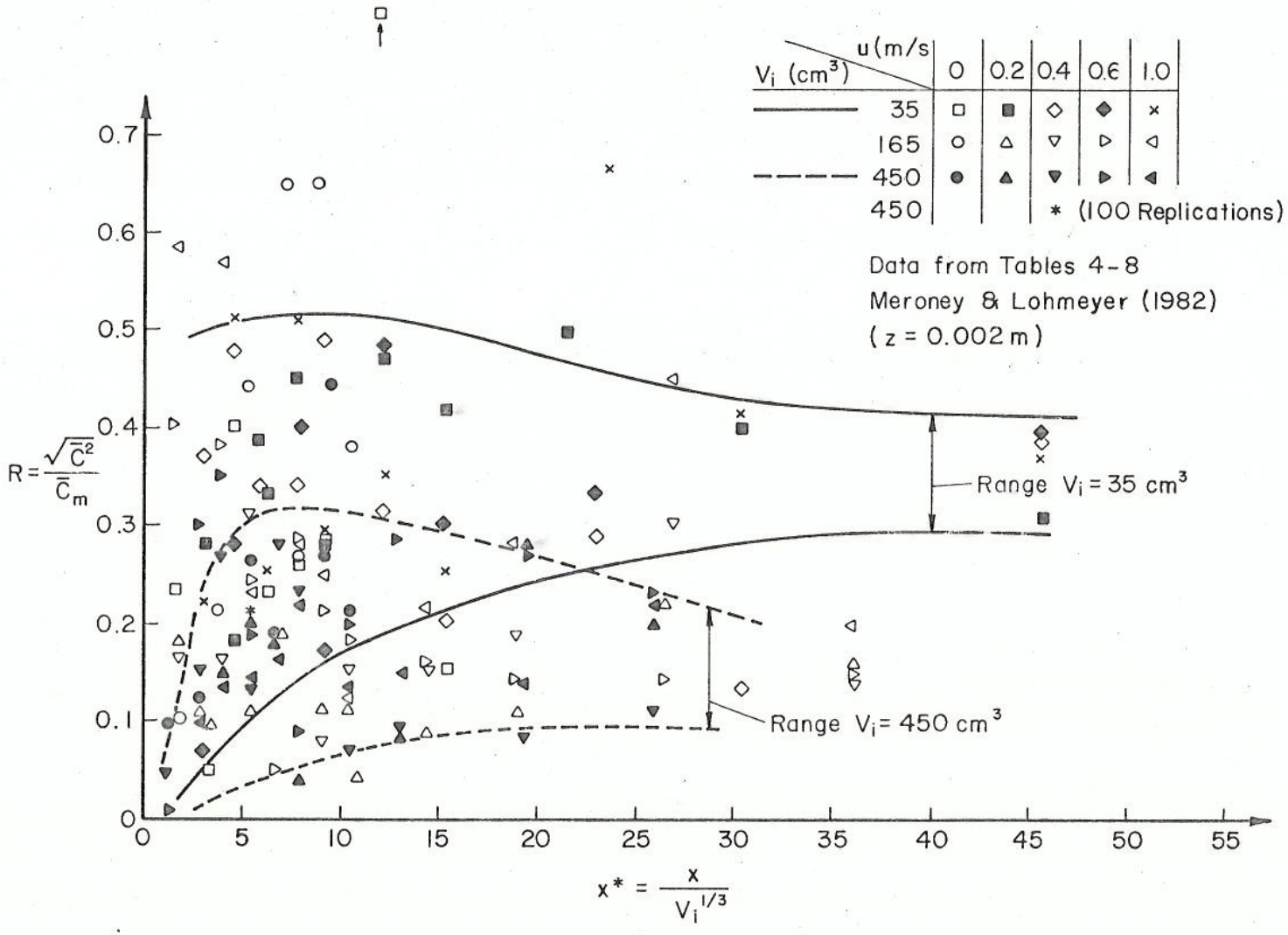

Figure 13. Concentration Variance Ratio versus Dimensionless Downwind Concentration

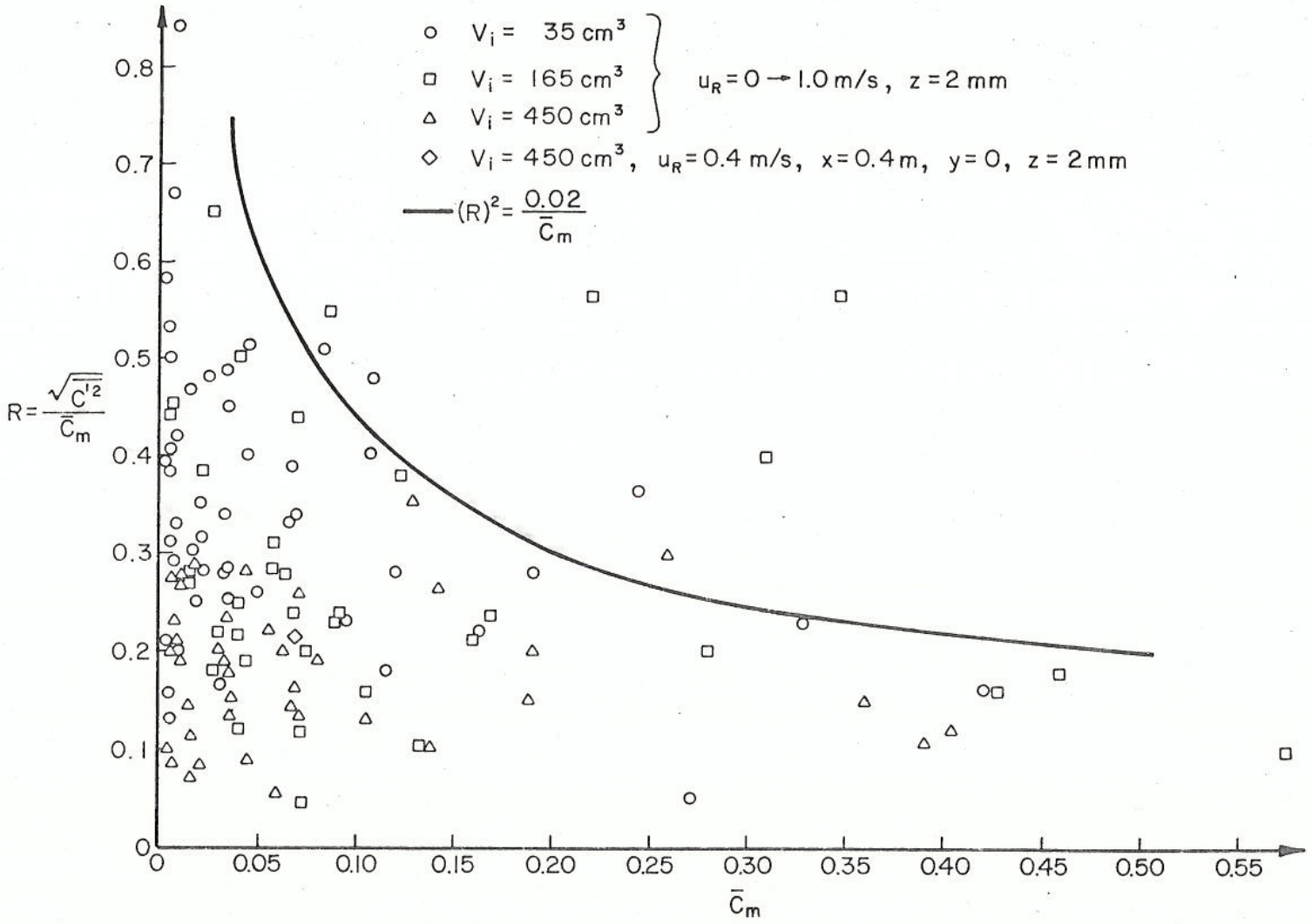

Figure 14. Concentration Variance Ratio versus Mean Concentration

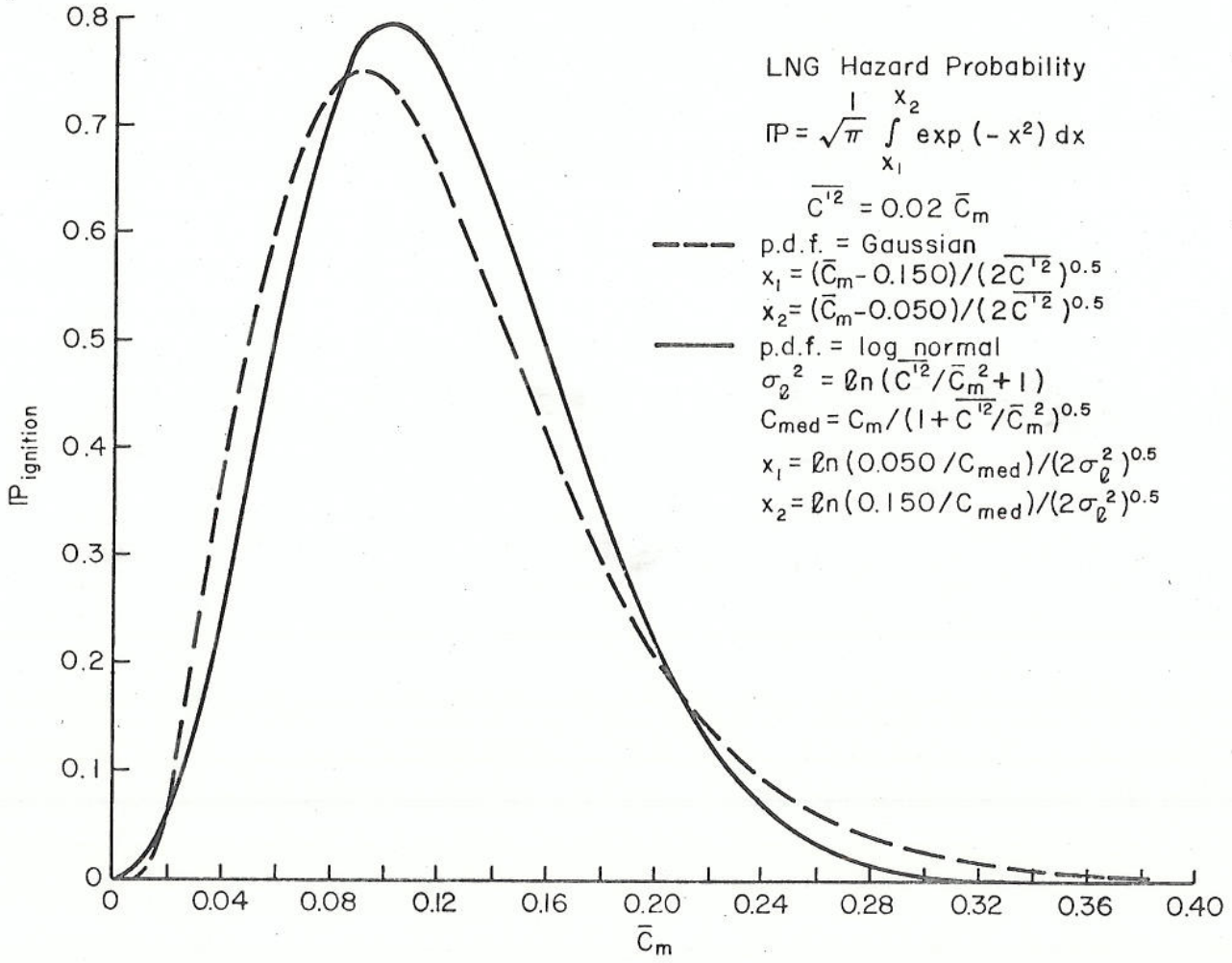

Figure 15. Probability of Ignition of LNG Vapor Cloud versus Mean Maximum Concentration

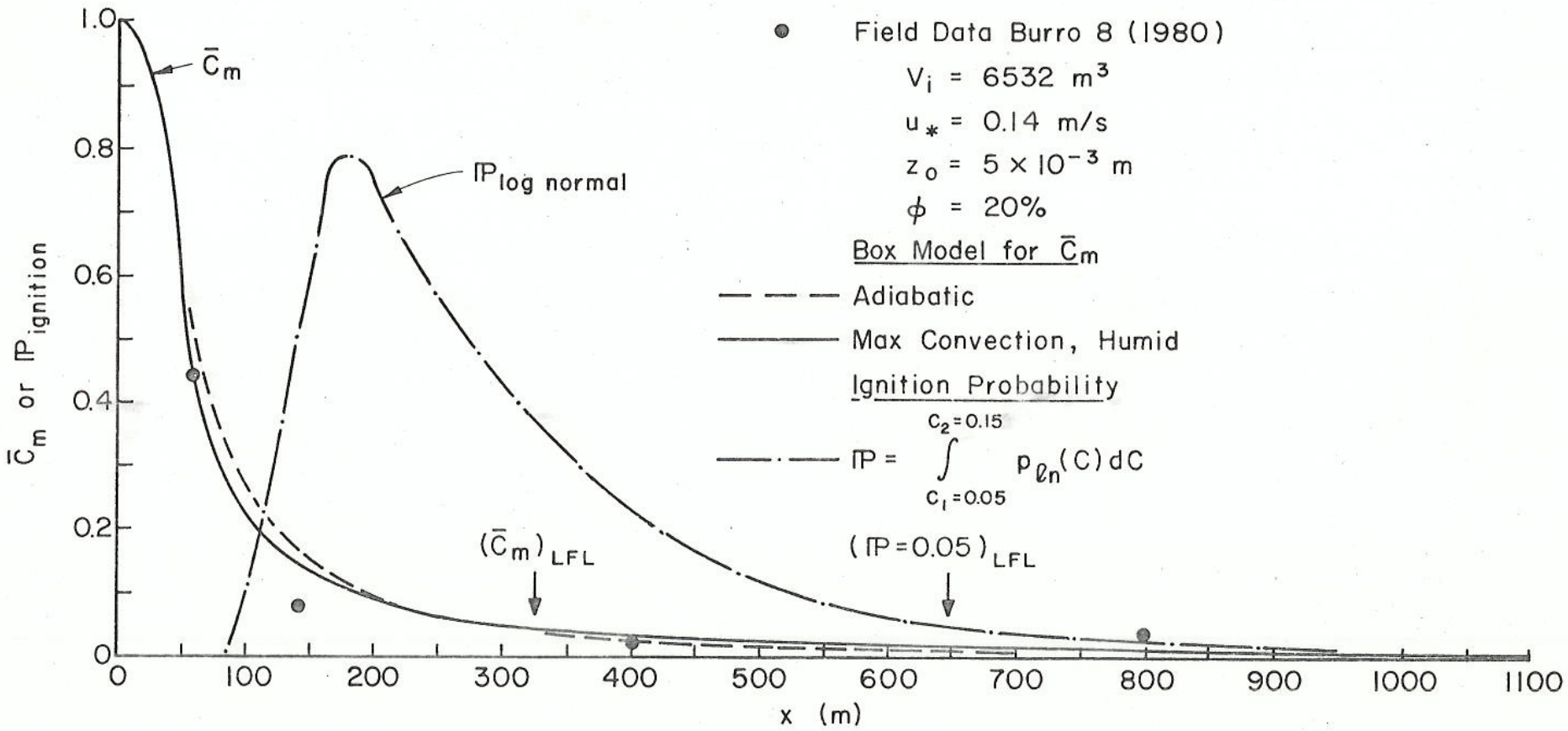

Figure 16. Ignition Probabilities during China Lake Burro 8 LNG Spill, $\overline{C_m}$ and P versus x (meters)

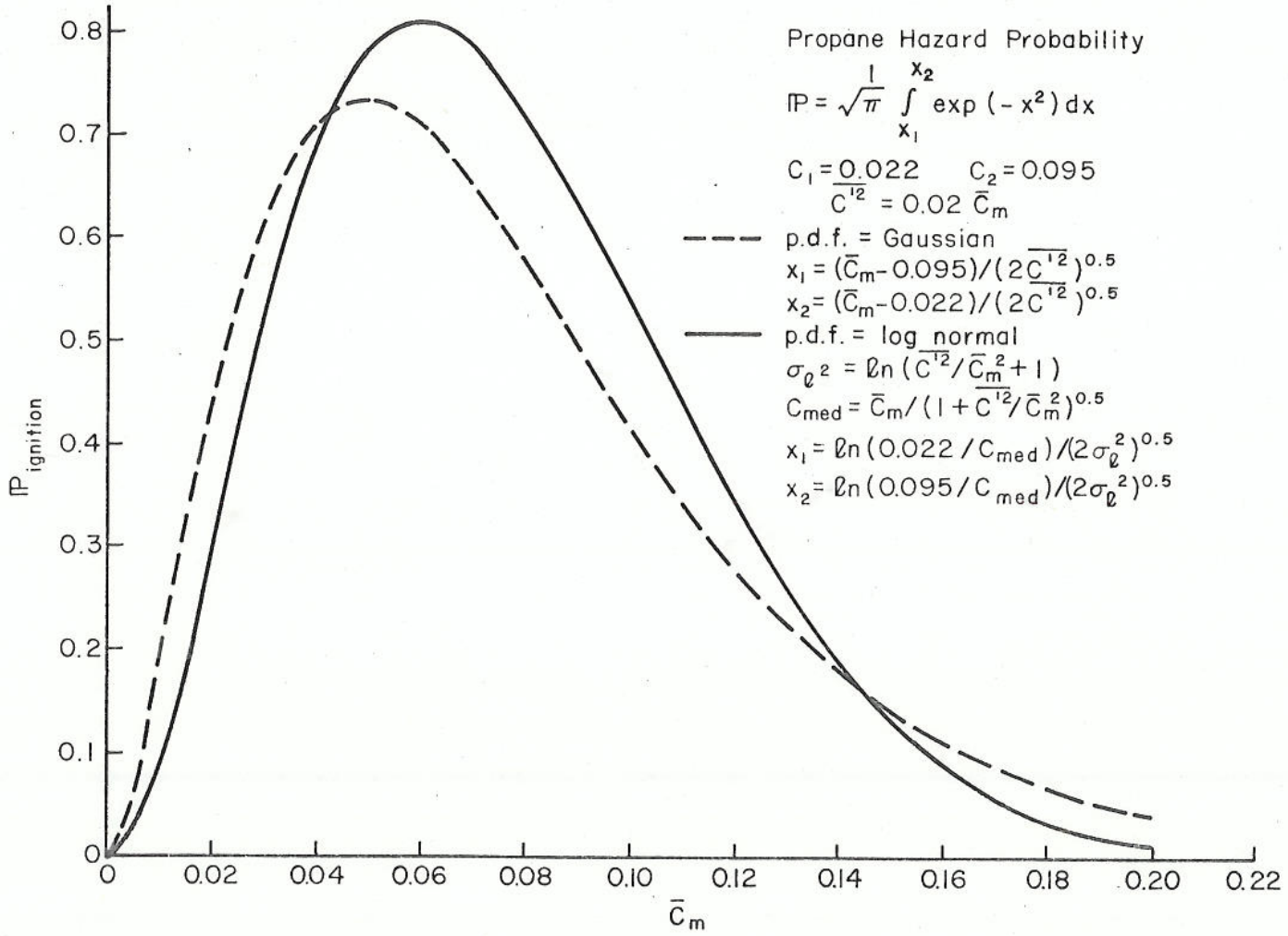

Figure 17. Probability of Ignition of Propane Cloud versus Mean Maximum Concentration